Percolation threshold in ultrathin titanium films determined by *in situ* spectroscopic ellipsometry

T. W. H. Oates,* D. R. McKenzie, and M. M. M. Bilek
School of Physics, A28, University of Sydney, N.S.W. 2006, Australia
(Received 6 April 2004; revised manuscript received 22 June 2004; published 8 November 2004)

We report on the use of *in situ* spectroscopic ellipsometry to determine the film thickness, optical constants, and growth rate for titanium films grown on silicon oxide by pulsed filtered cathodic vacuum arc. The growth rate and film thickness are shown to be highly controllable. We also report the results of simultaneous *in situ* spectroscopic ellipsometry and *in situ* conductivity measurements to independently verify the ability of both techniques to determine the percolation threshold. Percolation is shown to occur at a film thickness in the range 2.7 to 3.1(+/−0.1)nm. The ability of spectroscopic ellipsometry to accurately determine the void fraction in a thin film enables us to apply the percolation formalism based on a critical exponent to this system.

DOI: 10.1103/PhysRevB.70.195406 PACS number(s): 81.15.Aa, 68.55.Ac, 78.20.Ci, 73.61.At

I. INTRODUCTION

Precise control over the growth and structure of ultrathin films is of importance in modern technical applications. Applications of ultrathin films include coatings for magnetic storage technology,[1] multilayer coatings for tools,[2] thin conductive films on insulators for charge dissipation,[3] and low-emissivity coatings for energy efficient windows.[4] For many of these applications, the optimal film thickness occurs at or near the film percolation threshold where the film first has connected pathways. We have recently constructed a pulsed filtered cathodic vacuum arc for the purpose of depositing thin metal, carbon and ceramic films of precisely controlled thickness.[5] This precise control provides an opportunity for the study of nucleation and percolation phenomena occurring in the early stages of film growth.

The definition of the percolation threshold in a thin film is the first point in the growth process at which a connected pathway exists across the specimen. An equivalent definition is the point at which the size of connected clusters diverges. Methods which have been applied to the determination of the percolation threshold *in situ* include electrical resistivity measurements[6] and measurements of the real part of the complex dielectric function at optical frequencies[7] using spectroscopic ellipsometry (SE). The percolation thresholds determined by these methods have not yet been compared, nor has their relation to the above definition.

The optical properties of ultrathin films are markedly different from those of the bulk material. As a result it is not possible to independently determine the real and imaginary parts of the dielectric function, $\varepsilon_1(\lambda)$ and $\varepsilon_2(\lambda)$, together with the thickness by fitting SE data accumulated *in situ* using a fixed angle of incidence. Optical constants from the literature, typically measured for bulk materials, often result in erroneous values when used to determine the thickness of ultrathin films. Arwin and Aspnes have reported a method for determining the film thickness without prior knowledge of the optical properties of the film.[8] The method requires that the substrates possess a pronounced feature in the ellipsometric data. If the guessed thickness of a thin metallic film, deposited on such a substrate, is incorrect, the dielectric function of the film will show evidence of the substrate optical feature. The correct thickness can be determined by iteratively guessing the film thickness until the substrate related artefact is minimised. A comparison of the film thicknesses determined using this method with those determined using transmission electron microscopy has revealed the method to be highly accurate.[9]

Here we use the method of Arwin and Aspnes to determine the film thickness and optical constants of a growing titanium film using *in situ* SE. *In situ* measurements of conductivity are performed simultaneously. We use these results to compare the *in situ* resistivity and ellipsometry methods for the determination of the percolation threshold. Theory developed for a wide range of percolation phenomena is then applied to the growth of titanium films.

II. EXPERIMENT

A schematic diagram of the experimental arrangement is shown in Fig. 1. A 25 mm by A 75 mm silicon wafer with a thermally grown oxide of nominal thickness 500 nm was

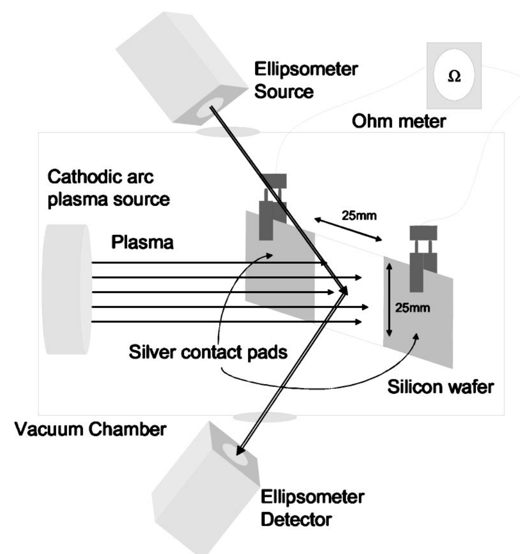

FIG. 1. Schematic of experimental arrangement showing *in situ* ellipsometer and *in situ* conductivity measurement.

 ©2004 The American Physical Society

used as a substrate. The substrate was plasma cleaned for 10 minutes by applying 20 μs, 4.5 kV pulses at a frequency of 1 kHz, to the substrate holder, initiating a glow discharge plasma in 0.66 Pa of argon gas. The high voltage was then switched off and titanium was deposited using a pulsed filtered cathodic vacuum arc system, which has been described in detail elsewhere.[5] The arc was ignited on a 99.99% pure titanium cathode and the peak arc current was approximately 3 kA. The arc pulse frequency was 0.1 Hz and the background gas pressure was less than 1×10^{-4} Pa. A magnetic solenoid filter was used to filter the plasma. A deposition rate of around 0.05 nm per pulse was expected from previous calibration with a surface profilometer.

The ellipsometer used for this study was a J.A. Woollam Co. M-2000 rotating compensator ellipsometer capable of collecting 390 wavelengths in a spectral range from 370–1000 nm. The ellipsometer heads were mounted on the deposition chamber at a nominal angle of incidence of 75 degrees (Fig. 1). Fused silica vacuum-sealed windows were used as entrance and exit ports for the incident and reflected light to minimize strain induced effects in the reflection signal. The substrate was modeled as a 1 mm silicon base layer with a SiO_2 layer on top. Optical data for both layers was taken from the Woollam database, originally sourced from the compilation of Palik.[10] The angle of incidence and the oxide film thickness were determined from this model to be 75.69° and 506.0 nm, respectively. Ellipsometric data was collected every ten arc pulses for 350 arc pulses. The deposition process was not interrupted for data acquisition.

The basic ellipsometric data are the ellipsometric parameters Δ and Ψ as a function of wavelength. These are defined by

$$\tan \Psi e^{i\Delta} = \boldsymbol{R}_p/\boldsymbol{R}_s, \tag{1}$$

where $\boldsymbol{R}_p$ and $\boldsymbol{R}_s$ are the complex Fresnel reflection coefficients for polarization states parallel (p) and perpendicular (s) to the plane of incidence. The reflection data is analysed by a regression analysis program, WVASE32™. A physical "slab" model is created, specifying the angle of light incidence, thickness and optical constants of various layers. WVASE32™ then calculates the mean squared error (MSE) for each (Δ,Ψ) pair, which is the sum of the squares of the difference between the measured and calculated data. A regression algorithm is then used to minimize the MSE by adjusting the values of one or more nominated parameters. If the final MSE is small and the parameter values are deemed acceptable, the model may be considered correct.

The conductivity of the growing metal film was simultaneously measured *in situ* by depositing metal electrodes onto the ends the silicon wafer, whilst leaving a 25 mm square uncoated region in the center (Fig. 1). The 500 nm surface oxide was sufficiently resistive to electrically isolate the electrodes from the c-Si substrate. The electrical resistance between the electrodes was measured using a Keithley 617 electrometer. Resistivity, ρ, is given by

$$\rho = Rwt/L, \tag{2}$$

where w, t and L are the width, thickness and length of the conductive region respectively. Since for a square w and L are equal, if the film thickness is known, the film resistivity can simply be calculated from the product of the measured resistance and film thickness.

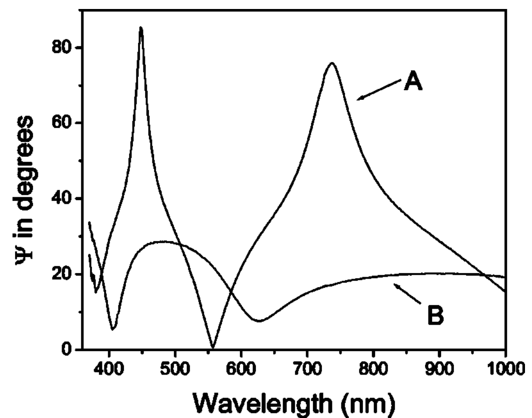

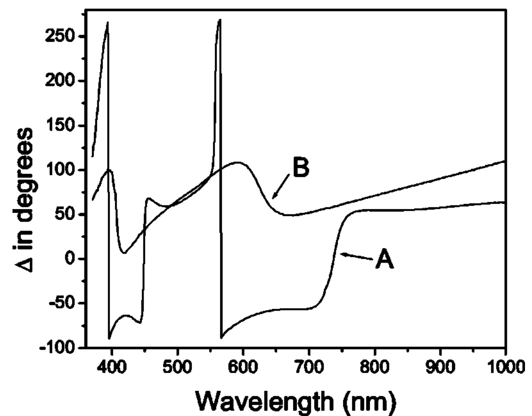

FIG. 2. (a) Ψ and (b) Δ values for pulsed FCVA titanium deposited on SiO_2/Si. (A) denotes the substrate reflection spectra and (B) the reflection spectra after 350 arc pulses.

III. RESULTS AND ANALYSIS

A. Thickness determination

Δ and Ψ values for the sputter cleaned substrate and after the titanium deposition are shown in Fig. 2. As more titanium is deposited on the oxide surface the extrema observed in the Ψ data, which are caused by optical interference in the oxide layer, become progressively weaker due to absorption in the metal layer. Modeling the film growth using the optical constants for bulk titanium gave poor results, indicating that the optical constants of the film deviated from those of the bulk. The film thickness and dielectric function of the thin films were therefore determined using the method described by Arwin and Aspnes.[8]

An example of the dielectric functions for a number of estimated film thicknesses is shown in Fig. 3 for data obtained after 100 arc pulses. The wavelength regions between 500 and 600 nm and near 400 nm exhibit a high sensitivity to thickness over the range of chosen thickness values due to

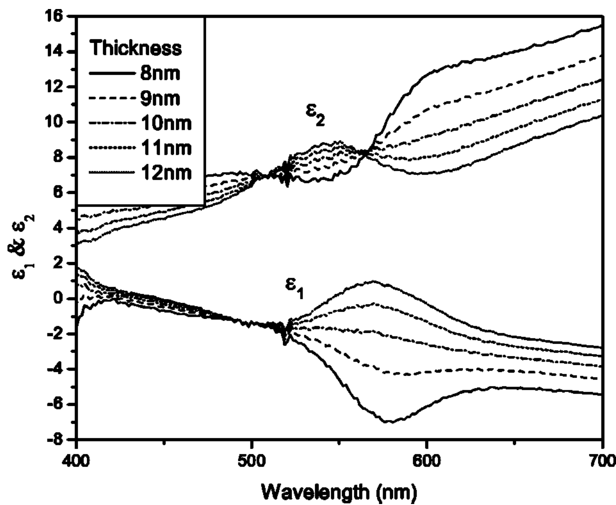

FIG. 3. Dielectric functions determined for different estimates of film thickness. The 10 nm estimate shows the smallest deviations at the location of the minima in the Ψ data from Fig. 2.

the influence of the substrate feature. A thickness value of 10 nm minimizes this effect (Fig. 3), and further refinement gave a film thickness of 9.7 ± 0.1 nm. When the film thickness is close to the correct thickness, the dielectric functions are smooth across the wavelength range under investigation, as would be expected for a metallic film in this wavelength region. Using this method, the determined film thickness is the thickness of a layer which includes the deposited material and voids. This is distinct from the mass thickness, which corresponds to the thickness of a layer containing the deposited material with no voids present.

Titanium film thickness as a function of the number of arc pulses, determined using the above method, is shown in Fig. 4. The deviation from linear growth rate below 5 nm is interpreted as being due to the presence of voids. Above this thickness, the results show good agreement with the expected linear deposition rate. A linear regression fit reveals a mass thickness deposition rate of 48.8 ± 0.2 pm per arc pulse with a regression coefficient of 0.9996. The data points between zero and 100 arc pulses were excluded from the fit due to the influence of voids. The deposition rate is in good agreement with the deposition rate of 50 pm per pulse, measured using profilometry.

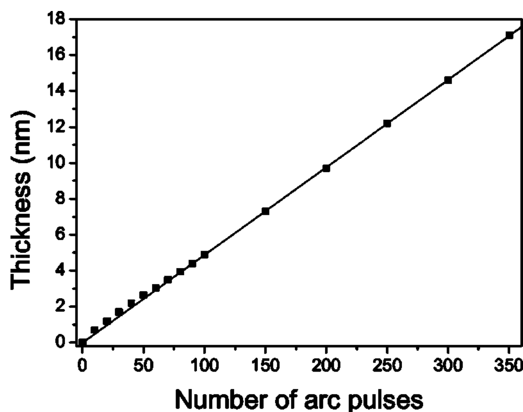

FIG. 4. Film thickness as a function of the number of arc pulses. The line is a linear fit to the data for points greater than 100 arc pulses. Note the deviation from constant growth rate below 100 arc pulses. Error bars are smaller than the data points.

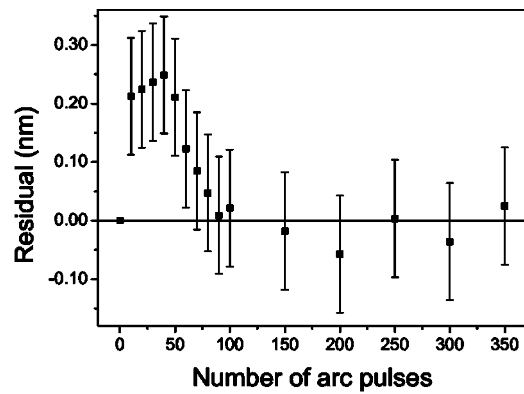

FIG. 5. Residual plot of the data in Fig. 4 showing the deviation from constant thickness growth rate in the early stages of the film growth.

Observation of the data points for film thickness below 3 nm reveals an above average film thickness growth rate. To explain this we note that it is generally observed that metal films grow on insulators in the Volmer-Weber, or island growth mode.[11] After nucleation, surface energy minimization drives the formation of metal islands. As more material is deposited the islands grow three dimensionally. In this first regime, the film thickness growth rate is higher than the mass thickness growth rate. As more material is deposited onto the surface, the voids between the islands infill. During this second regime, the film thickness growth rate is lower than the mass thickness growth rate. When complete surface coverage is achieved there is no mismatch between the surface energies of the growing film, and the substrate and films grow in a layer-by-layer or Frank–Van der Merwe growth. In this third regime, the film thickness increases at the same rate as the mass thickness.

The sensitivity of the SE thickness measurements allows us to identify these three regimes using the residual plot shown in Fig. 5. The data for this plot is the difference between the measured film thickness and the film thickness expected from the constant growth rate as determined from the fitted line in Fig. 4. For the first 40 arc pulses, the plot shows an elevated growth rate corresponding to nucleation and 3-dimensional island growth. From 40 to around 70 arc pulses, the film growth rate is less than the mass thickness growth rate. After this, the deposition rate becomes constant within the experimental error. Since the percolation threshold must occur when the voids are being in-filled (regime 2 above), we estimate that the percolation threshold occurs at a film thickness between 2.2 and 3.5($\pm$0.1) nm.

B. Percolation threshold determination

Figure 6 shows the dielectric functions of the films for a range of thicknesses. There is an increase in noise as the film thickness decreases and substrate related features cannot be

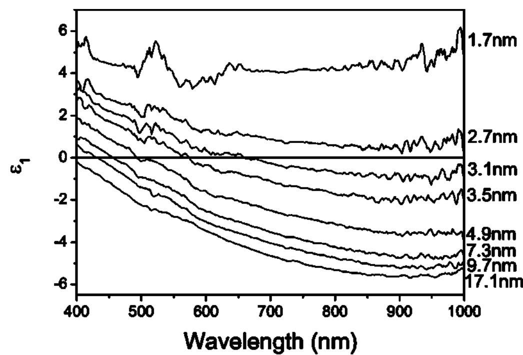

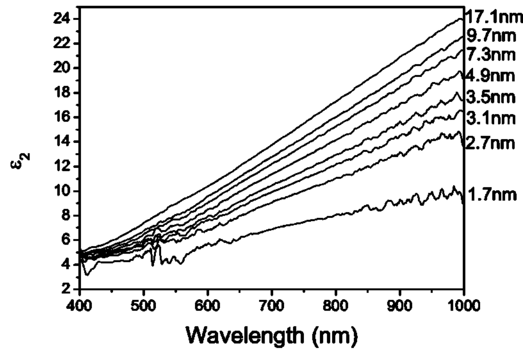

FIG. 6. Dielectric functions for thin titanium films determined using the method of Arwin and Aspnes (Ref. 8).

completely eliminated. Both ε_1 and ε_2 converge as the film thickness increases.

The Drude model for metallic conduction[12] is useful in assessing the point at which the dielectric function of the island film first shows metallic behavior. A criterion that can be applied is that the electrons be mobile enough to give a negative value of the real part of the dielectric function, ε_1. This occurs in the Drude model when the frequency lies in the range $1/\tau < \omega < \omega_p$ where τ is the relaxation time of electrons and ω_p is the plasma resonance frequency. From Fig. 6(a) this can be seen to occur for the thick titanium film (17.1 nm) in the visible and near infrared up to approximately 900 nm wavelength. The thin titanium films show a qualitatively similar behavior for thickness exceeding 2.7 nm but the negative ε_1 regime is moved to longer wavelengths. In the Drude model, this can be accommodated by an increase in the relaxation time, possibly a result of the reduced electron-electron interactions in an island film. The thickness at which ε_1 becomes negative is therefore associated with the percolation threshold of the film, which in this case occurs between 2.7 and 3.1($\pm$0.1) nm. SE therefore provides us with an independent, nondestructive method for determining the percolation threshold *in situ*.[7]

Figure 7 shows the resistivity of the titanium film measured simultaneously with the SE data used for the above analysis. The resistivity curve flattens out as the film thickness increases, to a value of $3.2\times10^{-6}\ \Omega$ m at a thickness of 17.1 nm. This is an order of magnitude higher than the value for bulk titanium of $4.3\times10^{-7}\ \Omega$ m published in the literature.[13] Metal films with thicknesses less than the mean free path of conduction electrons exhibit increased resistivity due to enhanced contribution from electron surface scattering. The mean free path for titanium at room temperature is of the order of 40 nm,[14] and we would therefore not expect the resistivity to approach the bulk value until the film reaches this thickness.

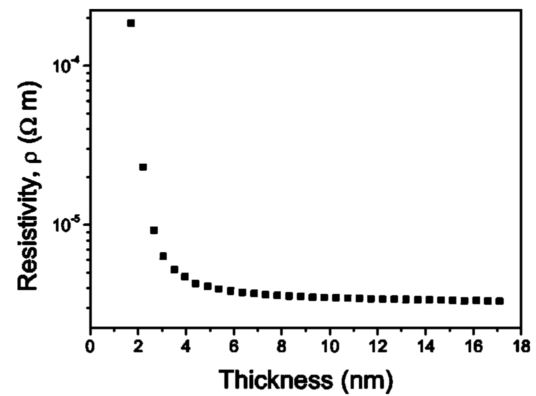

FIG. 7. Film resistivity as a function of film thickness for titanium.

Figure 7 shows that there is a dramatic decrease in the rate of change of the resistivity above a thickness of 3 nm. Conduction between islands in discontinuous ultrathin films is facilitated by electron tunnelling and conduction across the substrate surface.[15] As the percolation threshold is approached, conduction processes become increasingly dominated by bulk conduction mechanisms. A study by Maroof and Evans[6] on the determination of the percolation threshold for thin nickel and platinum films reports that the percolation threshold can be determined by finding the minimum value in a plot of film thickness, t, against resistance, R, multiplied by the square of the thickness (i.e., t vs Rt^2). Such a plot is shown in Fig. 8 using the data from Fig. 7. A derivative curve of this plot revealed the minimum to occur at 3.3$\pm$0.1 nm, which is outside the range predicted above using SE (2.7–3.1$\pm$0.1 nm). Both these values lie within the range predicted in the previous section by examining the deposition rate at low coverage (2.2–3.5$\pm$0.1 nm). Whilst the method of Maroof and Evans provides a simple experi-

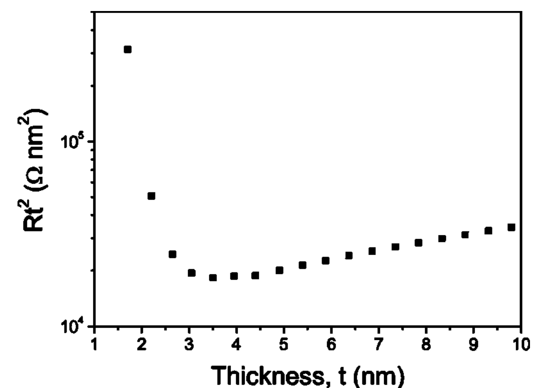

FIG. 8. Rt^2 as a function of film thickness. The minimum at 3.3 nm indicates the percolation threshold according to Maroof and Evans (Ref. 6).

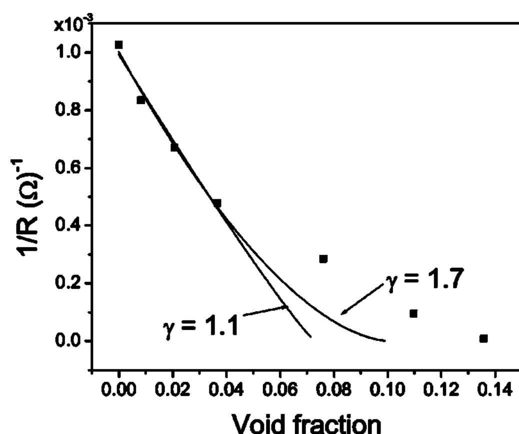

FIG. 9. Conductance $(1/R)$ as a function of void fraction. The fits are the percolation formula (3) using critical exponents of 1.1 and 1.7.

mental method for determining an approximate percolation threshold, there is little theoretical basis for the technique.

We investigate the validity of fitting the experimental data with a fundamental percolation formula[16]

$$\sigma = K[\Phi - \Phi_c]^\gamma, \quad (3)$$

where σ is the measured conductance, K is a constant, Φ is the void fraction of the film, Φ_c is the critical void fraction at the percolation threshold, and γ is the critical exponent. The variables γ, Φ, and σ in Eq. (3) can be determined experimentally as follows.

Previous experimental measurements of conductivity in discontinuous percolated films have yielded values for γ between 1.3 and 1.7 when analysed using Eq. (3).[17,18] In a recent unpublished experiment examining conductivity in a randomly perforated metal sheet we determined a γvalue of 1.1.[19] SE provides us with a unique method for determining the void fraction, Φ, of the film. Given that a constant mass of material is deposited on the substrate per pulse in our experiment, we can determine the void fraction from the ratio of the measured film thickness to the mass thickness. The conductance, σ, can be read directly from Fig. 7.

The conductance of films with void fractions between 0.14 and zero are shown in Fig. 9, along with fits using Eq. (3) for γ values of 1.1 and 1.7. These values for the critical exponent, γ, represent the two extremes of the critical exponent found experimentally for the case of conductivity percolation.[17,19] The parameters Φ_c and K were chosen as variables. The goodness-of-fit indicators, R^2, for the two curves were 0.981 and 0.988, respectively. The critical void fractions for the fits occur at 0.073 and 0.101 for γ values of 1.1 and 1.7, respectively. These correspond to total film thicknesses of approximately 2.6(±0.1) and 2.3(±0.1) nm, respectively. The latter value is outside the range of 2.7–3.1(±0.1) nm predicted using SE, however the former value lies within the limits of experimental uncertainty, providing support for a value of the critical exponent nearer to 1.1 than 1.7.

The percolation equation (3) only applies to conduction in the connected phase; that is for $\Phi \geqslant \Phi_c$ and specifically excludes conduction across void spaces. It therefore predicts zero conduction for $\Phi \leqslant \Phi_c$. Conduction between unconnected islands by mechanisms such as tunneling and thermionic emission is known to occur,[15] and these mechanisms become dominant near Φ_c. Inclusion of such conduction processes in a model for discontinuous films has been attempted in a recent publication by Bieganski.[20] The data point at the void fraction of 0.076 has therefore not been included in the percolation fit using Eq. (3). These additional conduction processes can be included in a percolation formalism by the inclusion of an additional term dependent on Φ, so that Eq. (3) has the form

$$\sigma = K[\Phi - \Phi_c]^\gamma + f(\Phi). \quad (4)$$

The inclusion of the additional term may account for the discrepancy between the percolation thickness determined using Eq. (3) and that measured experimentally.

IV. CONCLUSION

We conclude that *in situ* spectroscopic ellipsometry can precisely determine the thickness, and hence the deposition rate of ultrathin metal films using the method described by Arwin and Aspnes. Spectroscopic ellipsometry also provides us with a method of finding the percolation threshold in metal films by locating the thickness at which the real part of the dielectric function first becomes negative. Using this method the film thickness at the percolation threshold for titanium lies in the range 2.7 to 3.1(±0.1) nm. An independent measurement using *in situ* resistance measurements yielded a value of 3.3(±0.1) nm, which is outside this range. This result questions the choice of the minimum in Rt^2 as giving a precise value of the percolation thickness.

Application of a percolation model based on the accepted critical exponent for conductivity in systems containing voids yielded a range of percolation film thicknesses from 2.3 to 2.6(±0.1) nm, the latter value lying within range measured by spectroscopic ellipsometry when the experimental uncertainty is considered. This result gives confidence that the percolation model applies to this system, a result only made possible because spectroscopic ellipsometry provides a definitive method of determining the void fraction in ultrathin films.

ACKNOWLEDGMENTS

The authors would like to thank John Pigott, Bee Kwan Gan, and Richard Tarrant for assistance. Financial assistance from Australian Research Council and the University of Sydney Sesqui Scheme is gratefully acknowledged.

*Corresponding author. Present address: Forschungszentrum Rossendorf e.V. P.O. Box 510119, 01314 Dresden, Germany. Email address: t.oates@fz-rossendorf.de

[1] A. Anders, W. Fong, A. V. Kulkarni, F. W. Ryan, and C. S. Bhatia, IEEE Trans. Plasma Sci. **29**, 768 (2001).
[2] D. R. McKenzie, R. N. Tarrant, M. M.M. Bilek, T. Ha, J. Zou, W. E. McBride, D. J.H. Cockayne, N. Fujisawa, M. V. Swain, N. L. James, J. C. Woodard, and D. G. McCulloch, Diamond Relat. Mater. **12**, 178 (2003).
[3] T. W. H. Oates and M. M. M. Bilek, J. Appl. Phys. **92**, 2980 (2002).
[4] R. J. Martin-Palma, L. Vazquez, J. M. Martinez-Duart, and A. Malats-Riera, Sol. Energy Mater. Sol. Cells **53**, 55 (1998).
[5] T. W. H. Oates, J. Pigott, D. R. McKenzie, and M. M. M. Bilek, Rev. Sci. Instrum. **714**, 4750 (2003).
[6] A. I. Maroof and B. L. Evans, J. Appl. Phys. **76**, 1047 (1994).
[7] H. V. Nguyen, I. An, and R. W. Collins, Phys. Rev. B **47**, 3947 (1993).
[8] H. Arwin and D. E. Aspnes, Thin Solid Films **113**, 101 (1984).
[9] L. Ryves, M. M. M. Bilek, T. W. H. Oates, R. N. Tarrant, D. R. McKenzie, F. A. Burgmann, and D. G. McCulloch, *Proceedings of EMRS 2004*, Strasbourg, France, 2004 [Thin Solid Films (to be published)].
[10] E. D. Palik, *Handbook of Optical Constants of Solids* (Academic, Orlando, 1985).
[11] M. Ohring, *Materials Science of Thin Films; Deposition and Structure*, 2nd ed. (Academic, San Diego, 2002).
[12] P. Drude, Ann. Phys. (Leipzig) **1**, 566 (1900).
[13] C. Kittel, *Introduction to Solid State Physics*, 7th ed. (Wiley, New York, 1996).
[14] H. -D. Liu, Y. -P. Zhao, G. Ramanath, S. P. Murarka, and G. -C. Wang, Thin Solid Films **384**, 151 (2001).
[15] T. J. Coutts, *Electrical Conduction in Thin Metal Films* (Elsevier, Amsterdam, 1974).
[16] L. Benguigui, Phys. Rev. Lett. **53**, 2028 (1984).
[17] K. Sieradzki, K. Bailey, and T. L. Alford, Appl. Phys. Lett. **79**, 3401 (2001).
[18] A. Okazaki, K. Horibe, K. Maruyama, and S. Miyazima, Phys. Rev. E **61**, 6215 (2000).
[19] M. Verdon (private communication).
[20] P. Bieganski, E. Dobierzewska-Mozrzymas, E. Pieciul, and G. Szymczak, Vacuum **74**, 211 (2004).